Rapid Communications

Discommensuration-driven superconductivity in the charge density wave phases of transition-metal dichalcogenides

Chuan Chen,[1,2] Lei Su,[3] A. H. Castro Neto,[1,2] and Vitor M. Pereira[1,2]
[1]*Centre for Advanced 2D Materials and Graphene Research Centre, National University of Singapore, Singapore 117546*
[2]*Department of Physics, National University of Singapore, Singapore 117542*
[3]*Department of Physics, University of Chicago, Chicago, Illinois 60637, USA*

(Received 20 June 2018; revised manuscript received 18 October 2018; published 18 March 2019)

We introduce a McMillan-Ginzburg-Landau theory to describe the cooperative coexistence of charge density and superconducting order in two-dimensional crystals. With a free energy that explicitly accounts for the competition between commensurate and incommensurate ground states, we are able to map the transition between these phases and monitor the development of discommensurations in the near-commensurate regime. Attributing the enhancement of superconducting order to density wave fluctuations, we propose a coupling scheme that yields a phase diagram in qualitative agreement with experiments in conducting transition-metal dichalcogenides. The model predicts the development of nonuniform superconductivity similar to that arising from a pair density wave, with a spatial texture driven by the underlying charge density wave fluctuations.

DOI: 10.1103/PhysRevB.99.121108

Recent experiments suggest a relation between emergent superconductivity in doped transition-metal dichalcogenides (TMDs) and fluctuations of their charge density wave (CDW) order [1–4]. The archetype example of $1T$-$TiSe_2$ ($TiSe_2$ in short) displays superconductivity (SC) amidst CDW order as soon as the nature of the latter changes from commensurate (C) to incommensurate (IC) under electron doping [1,5–7] or pressure [6,8], either in bulk or two-dimensional (2D) samples [1,9]. SC is limited to a dome over a small range of the external parameter x (doping or pressure) in the T-x phase diagram. Since CDW correlations persist in the SC phase [10] and the dome is centered at the putative quantum critical point of the commensurate CDW (C-CDW) phase, it has been suggested that SC might arise (or be enhanced) as a result of CDW fluctuations [4,11,12].

The basic excitation of a C-CDW is called *discommensuration* (DC) [13], a localized defect (domain wall) where the phase of the order parameter jumps by $2\pi\nu$, with ν the commensurability fraction [13–15]. DCs have been observed in $TiSe_2$ by scanning tunneling microscopy (STM) [2,3] above the optimal SC transition temperature ($T_{SC}^{max} \simeq 4$ K), and are implied by inelastic scattering [7]. This suggests that the CDW converts from C to IC through a near-commensurate (NC) regime characterized by a finite density of DCs, similarly to the cases of $2H$-$TaSe_2$ [13] or $1T$-TaS_2 [16].

Although the range $T < T_{SC}$ remains unexplored by STM, Little-Parks magnetoresistance oscillations [17] observed in $TiSe_2$ films [1] were interpreted as a result of supercurrents constrained by an underlying periodicity tied to the CDW background. STM observations of enhanced density of states within DCs [2] indirectly support this. Moreover, the onset of a DC network introduces new low-energy phonons [18,19] that can couple to electrons and induce a Cooper instability [20]. Both ingredients suggest that the underlying theory must tie SC to both fluctuations and the domain structure of the electronic CDW.

To investigate the potential role of CDW fluctuations in either inducing or enhancing the SC order, we propose an extension of McMillan's Ginzburg-Landau framework for the CDW in layered TMDs [13,21]. It incorporates a SC order parameter coupled to the electronic density via DCs. In the vicinity of the C-IC transition (the NC regime), the predicted phase diagram reproduces the experimental one in $TiSe_2$ with no fine tuning of parameters (all $\sim$1). The nature of the SC phase is interesting and novel: The model implies nonuniformity in the NC regime close to T_{sc} and, with decreasing temperature, SC order might sequentially percolate from 0D to 1D to 2D.

CDW order. McMillan established the approach to the C-IC transition in terms of a free-energy functional with a complex order parameter [13,21]. Although the approach is general, the relevant nonlinear and umklapp terms depend on the particular ordering vectors and commensurability condition [21]. To be specific, we consider here the case of $TiSe_2$ since its small carrier density makes it an easily tunable system [1,6,7]. Both bulk [22] and monolayer [23] $TiSe_2$ undergo a second-order phase transition to the C-CDW phase characterized by the formation of a 2×2 superlattice in the 2D planes. The experimentally measured density modulation $\delta\rho(\mathbf{r})$ is contributed by three plane waves with wave vectors $\mathbf{Q}_j^C \equiv \mathbf{G}_j/2$, where $\mathbf{G}_j$ ($j = 1, 2, 3$) are primitive reciprocal vectors related by C_3 rotations [22]. As the in-plane ordering is the same in both the bulk and monolayer [23], we neglect the interlayer coupling and focus on the doping-temperature phase diagram of a $TiSe_2$ monolayer [1,7]. We ignore electronic disorder [24], as appropriate for gate-induced doping in encapsulated few-layer systems [1], or doping by Cu intercalation that donates conduction electrons without a visible

disruption of the electronic band structure [5,12]. Following the approach of Refs. [21,25,26], we define the complex CDW order parameters, $\psi_j(\mathbf{r}) \equiv \varphi_j(\mathbf{r})e^{i\theta_j(\mathbf{r})}$, according to

$$\delta\rho(\mathbf{r}) \equiv \sum_j e^{i\mathbf{r}\cdot\mathbf{Q}_j^C}\psi_j(\mathbf{r}) + \text{c.c.}, \tag{1}$$

where $\psi_j(\mathbf{r})$ encodes deviations from the C state. To describe the IC phase, we introduce the wave vectors $\mathbf{Q}_j^I$ that parametrize a uniform IC-CDW with the same symmetry. In line with experiments [20], we take $\mathbf{Q}_j^I = (1+\delta)\mathbf{Q}_j^C$, where δ quantifies the incommensurability, and further define $\mathbf{q}_j^I \equiv \mathbf{Q}_j^I - \mathbf{Q}_j^C$, $q^I \equiv |\mathbf{q}_j^I| = \delta|\mathbf{Q}_j^C|$.

The free-energy density consists of a conventional Ginzburg-Landau portion,

$$f_0(\mathbf{r}) \equiv A\sum_j |\psi_j|^2 + B\sum_j \left|\left(i\nabla_j + \mathbf{q}_j^I\right)\psi_j\right|^2 + G\sum_j |\psi_j|^4, \tag{2a}$$

where the B term favors a solution $\psi_j(\mathbf{r}) \propto e^{i\mathbf{q}_j^I\cdot\mathbf{r}}$ that distorts $\delta\rho(\mathbf{r})$ towards an IC state [27]. The quadratic coefficient is assumed to vanish linearly at a critical temperature $A \equiv t \propto T - T_{\text{ICDW}}$, t being the reduced temperature. The presence of noncollinear waves contributing to $\delta\rho(\mathbf{r})$ entails additional terms in the free energy to fourth order [21,25]. Symmetry dictates them to be [20]

$$f_1(\mathbf{r}) \equiv -\frac{E}{2}\sum_j\left(\psi_j^2 + \psi_j^{*2}\right) - \frac{3D}{2}(\psi_1\psi_2\psi_3 + \text{c.c.}) - \frac{M}{2}\sum_j(\psi_j\psi_{j+1}^*\psi_{j+2}^* + \text{c.c.}) + \frac{K}{2}\sum_{i\neq j}|\psi_i\psi_j|^2. \tag{2b}$$

The total CDW free energy reads $\mathcal{F}_{\text{CDW}} \equiv \int[f_0(\mathbf{r}) + f_1(\mathbf{r})]d\mathbf{r}$. The subscript j runs cyclically over $\{1,2,3\}$ in all our expressions (e.g., $\psi_5 \equiv \psi_2$). Physically, the last three terms in Eq. (2b) reflect the electrostatic cost incurred by the superposition of distinct density waves [28]. The E term represents the *lock-in* energy since it lowers the total energy of a C-CDW but averages out for an IC-CDW, thereby favoring the former.

Equation (2b) induces harmonics of any IC-CDW characterized by $\psi_j \propto e^{i\mathbf{q}_j\cdot\mathbf{r}}$, implying that the equilibrium IC state consists of a linear combination of all compatible harmonics and making the analytical minimization of $\mathcal{F}_{\text{CDW}}$ a formidable task. We tackle the problem numerically with a systematic expansion of the order parameter, as pioneered by Nakanishi *et al.* [26,29,30]. The method amounts to expanding each $\psi_j(\mathbf{r})$ in terms of $e^{i\mathbf{q}_j\cdot\mathbf{r}}$ and all the two-dimensional harmonics spawned by the nonlinear terms in Eq. (2b) [20]. This converts $\mathcal{F}_{\text{CDW}}$ from a functional of $\psi_j(\mathbf{r})$ into a function of a countable set of amplitudes $\Delta_{j;lmn}$ and wave vectors $\mathbf{q}_{j;lmn}$ of the different harmonics. The equilibrium solution follows from minimizing $\mathcal{F}_{\text{CDW}}$ with respect to these parameters as well as $\mathbf{q}_j$ itself. We take $\mathbf{q}_j \| \mathbf{q}_j^I$, and introduce $\eta \equiv |\mathbf{q}_j|/q^I$ that determines if the solution is a C-CDW ($\eta = 0$), a uniformly IC-CDW ($\eta = 1$), or in between (NC-CDW).

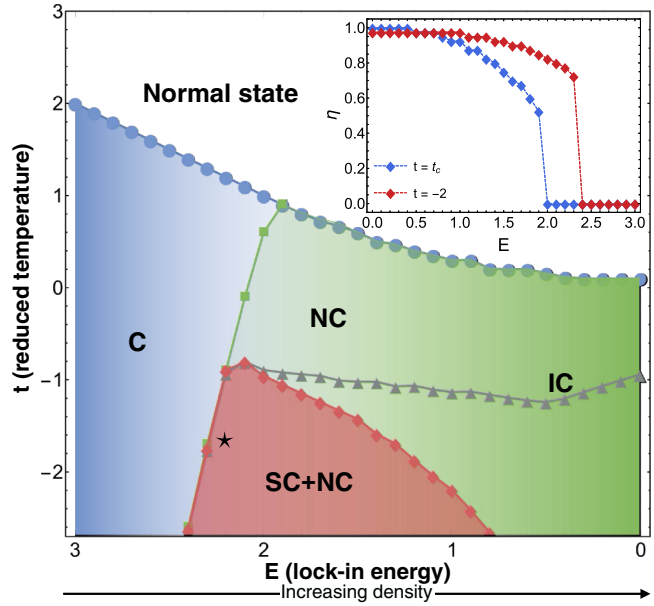

FIG. 1. Phase diagram obtained by minimizing $\mathcal{F}_{\text{CDW}}$. Labels C, NC and IC stand for commensurate, near-commensurate and homogeneously incommensurate CDW phases, respectively. When $\mathcal{F}_{\text{CDW}} < 0$, the system is in a CDW state and the C phase corresponds to $\eta = 0$. The green line represents the C-IC boundary $E_c(t)$. The red line indicates the boundary of the SC phase including the linear E dependence in the CDW-SC coupling a_s of Eq. (3) ($a_1 = 500E$); it becomes the gray line if a_s is E independent ($a_1 = 500 \times 2.1$). The inset shows the equilibrium η at t_c (first-order transition) and at low temperature.

CDW phase diagram. As we are only interested in scrutinizing the C-IC transition, we map the phase diagram in the E-t plane fixing the remaining parameters to $A = t$, $K = G = 2B(q^I)^2 = -2D = 2M = 2$ [20]. Without any fine tuning, this choice already allows us to concentrate on the C-IC boundary shown in Fig. 1 and drive the transition via E, which controls the energy gain of having a C-CDW. Physically, a *smaller* E can be mapped to *larger* electron densities because (i) phenomenologically, electron doping reduces the stability of the C state in favor of an IC one [1,2,7], and (ii) the lock-in gain reflects the condensation energy of the C-CDW phase in a microscopic description, and the latter has been shown to decrease with doping in the excitonic theory for the C-CDW in $TiSe_2$ [20,31–33]. For this reason, the horizontal E axis in the figure is reversed so that electron densities increase from left to right.

The phase diagram in Fig. 1 exhibits the anticipated stability of the C state at large E (low density) and its suppression below a critical, temperature-dependent lock-in parameter $E_c(t)$. Note that the critical temperature $t_c(E)$ decreases when progressing from the C to the IC state, in agreement with the experimental trend [1,7]. Likewise in agreement is the abrupt loss of the C phase indicated by the steep slope of the line $E_c(t)$. In light of our earlier definition of t, the asymptotic tendency $t_c(E \to 0) \approx 0$ means that $T_c \to T_{\text{ICDW}}$, or that, as expected from (2a), a uniform IC state is ultimately preferred in the absence of lock-in energy. The inset shows the equilibrium value of η at the critical temperature of the

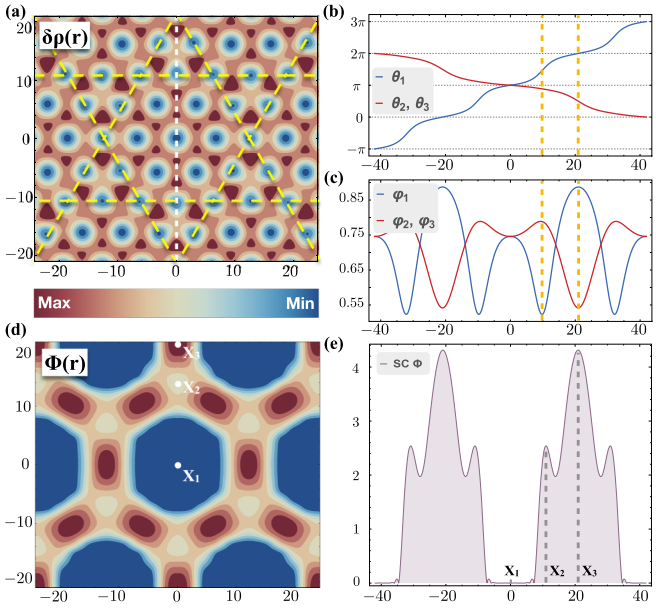

FIG. 2. (a) Real-space plot of the density profile $\delta\rho(\mathbf{r})$ at $E = 2.2$, $t = -1.7$ (in units of $\sqrt{3}a/2\pi$, with a the lattice constant). The yellow-dashed lines mark the places where the phase of each CDW order parameter, $\psi_j(\mathbf{r})$, jumps by π. (b) and (c) respectively show the phase and amplitude of $\psi_j(\mathbf{r})$ along the white vertical cut marked in (a). (d) The SC order parameter $\Phi(\mathbf{r})$ in the same region as (a). (e) $\Phi(\mathbf{r})$ along the vertical cut marked in (a).

normal-CDW transition and at low temperatures: It grows towards $\eta \approx 1$ with decreasing E, implying that the dominant wave vectors contributing to $\delta\rho(\mathbf{r})$ increasingly approach the reference IC vector $\mathbf{Q}_j^I$.

Knowledge of η is insufficient to characterize the rich spatial texture of the charge modulation which depends on the detailed harmonic content that minimizes $\mathcal{F}_{\rm cdw}$ [Supplemental Eq. (S6)]. Figure 2(a) shows $\delta\rho(\mathbf{r})$ at the representative point close to the C-CDW boundary marked by $\star$ in Fig. 1. Figures 2(b) and 2(c) show line cuts of the phase and amplitude of the order parameters $\psi_j(\mathbf{r}) \equiv \varphi_j(\mathbf{r})e^{i\theta_j(\mathbf{r})}$ along the vertical dashed line in Fig. 2(a). The phase $\theta_j(\mathbf{r})$ displays a stepwise variation with periodic slips of π. Since (1) implies that regions where $\theta_j(\mathbf{r}) \approx 0 \bmod \pi$ are commensurate with the Bravais lattice, the spatial profile of the phase reveals an equilibrium state characterized by domains of approximately C-CDW separated by DCs of π. This NC regime replicates the characteristics of CDW domain walls investigated by STM slightly above $T_{\rm sc}$ in $TiSe_2$ [2,3].

Adapting Eq. (2b) to a general commensurability condition $\mathbf{Q}^C = \nu\mathbf{G}$ with ν a rational number ($\nu = 1/2$ for $TiSe_2$), one obtains a corresponding domain structure with phase steps of $2\pi\nu$ across domain boundaries [14,18,25,26,30]. In 1D phase-only reductions of this problem [$\varphi_j(\mathbf{r}) = \text{const}$], the saddle-point condition for $\mathcal{F}_{\rm CDW}$ becomes a sine-Gordon equation [14,18] and DCs correspond to its soliton solutions. Even though our problem of interest is two dimensional, Eq. (1) still consists of a linear combination of 1D CDW modulations along each $\mathbf{G}_j$. It is thus not surprising that each $\theta_j(\mathbf{r})$ in Fig. 2(b) retains a solitonlike nature.

The DCs form a 2D kagome superlattice overlaying the C-CDW, as highlighted by the yellow-dashed contours in Fig. 2(a). For a general commensurability fraction ν, the period of the DC network is $L = 2\pi\nu/(\eta q^I) = \sqrt{3}a/(\eta\delta)$, where a is the lattice constant of the crystal in the normal phase.

Note that the amplitude of $\psi_i(\mathbf{r})$ is also significantly modulated: Fig. 2(c) shows it can drop more than 30% at each DC. The high variational freedom possible in our harmonic expansion permits the CDW to distort in order to minimize both the lock-in and gradient terms of $\mathcal{F}_{\rm CDW}$. The solution thus acquires both C *and* IC features, consisting of domains with a nearly flat phase and high amplitude (C-CDW), joined by domain boundaries where the amplitude drops to lessen the cost in deviating from commensurability, and the phase jumps so that, on spatial average, $\langle\theta_j(\mathbf{r})\rangle \approx \mathbf{q}_j^I \cdot \mathbf{r}$ (IC-CDW).

Coupling to superconductivity. It is natural to expect these DCs to couple strongly with the SC order parameter: On the one hand, the development of a DC superlattice as in Fig. 2(a) introduces new low-energy phonons [18–20] that might enhance any intrinsic phonon-mediated pairing tendency. On the other hand, DCs are but CDW fluctuations. While both phase and amplitude fluctuations are gapped in the C regime [15], the transition to the NC state releases them to potentially favor SC through fluctuation-induced pairing.

As a minimal approach to describe the interplay between the two orders, we propose extending the conventional [34] Ginzburg-Landau free energy associated with the SC order parameter $\Phi(\mathbf{r})$ by writing

$$\mathcal{F}_{\rm sc} \equiv \int [a_s(T, \nabla\psi_j)|\Phi|^2 + b_s|\nabla\Phi|^2 + c_s|\Phi|^4]d\mathbf{r}. \quad (3)$$

Making a_s a function of $\nabla\psi_j$ permits the enhancement of SC by deviations from a C-CDW. To lowest order in the interaction and inhomogeneity, a_s should have the form $a_s = a_0 - a_1\sum_j|\nabla\psi_j|^2$, where a_0 is the conventional quadratic coefficient ($a_0 \propto T - T_0$ if there are sources of pairing other than CDW fluctuations, which could lead to SC below some temperature T_0) and $a_1 > 0$ so that SC is stabilized within regions of fluctuating C order (we take a_1 to be T independent). This captures, phenomenologically, fluctuation-*induced* ($a_0 = \text{const}$) and fluctuation-*enhanced* ($a_0 \propto T - T_{\rm SC}$) pairing, as well as the spatial enhancement of the electronic DOS at DCs [2].

The total free energy is now $\mathcal{F} = \mathcal{F}_{\rm CDW} + \mathcal{F}_{\rm SC}$ and the coupling in (3) requires a self-consistent solution for both $\psi_j(\mathbf{r})$ and $\Phi(\mathbf{r})$. As in $TiSe_2$, $T_{\rm CDW} \simeq 60$ K and $T_{\rm SC} \simeq 4$ K $\ll T_{\rm CDW}$ [1,5,7,8], the CDW is already well developed when SC emerges. This justifies solving the two problems independently, where $\mathcal{F}_{\rm SC}$ is minimized subject to a passive CDW background $\psi_j(\mathbf{r})$ determined by $\mathcal{F}_{\rm CDW}$ [although we note that the back-influence of a finite $\Phi(r)$ on $\psi_j(r)$ implied by Eq. (3) increases CDW fluctuations via DCs so that SC and DCs mutually stabilize each other]. A representative result [20] is shown in Fig. 2(d) for the CDW solution in Fig. 2(a) [35]. The most significant feature is the nonuniformity of $\Phi(\mathbf{r})$ that follows the spatial texture of the DC network. The section plotted in Fig. 2(e) shows there is no SC within the C domains [$\Phi(\mathbf{x}_1) = 0$] but only at and near the DCs, and that

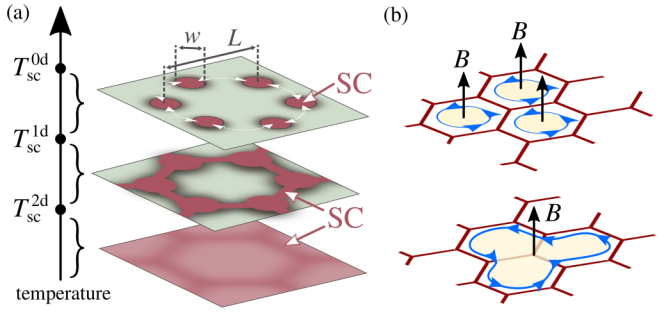

FIG. 3. (a) Schematic of the distinct nonuniform SC regimes spatially correlated with the DC network: nucleation and expansion of the SC order parameter ($T_{SC}^{1D} < T \leqslant T_{SC}^{0D}$), percolation ($T_{DC}^{2D} < T \leqslant T_{SC}^{1D}$), and finite everywhere. See Supplemental Fig. S4 for actually calculated textures. (b) Illustration of how the connectivity in the percolation regime constrains the vortex structure, with impact in the magnetic response.

SC is reinforced when two DCs overlap at the vertices of the kagome, $\Phi(\mathbf{x}_3) \approx 2\Phi(\mathbf{x}_2)$.

Interestingly, it is clear from how $\nabla\psi_j$ enters the quadratic coefficient a_s in Eq. (3) that the development of SC in the NC regime can take place in three stages with decreasing temperature: (i) It begins at T_{SC}^{0D} with the nucleation of isolated SC dots at the kagome vertices, as illustrated at the top of Fig. 3(a) that depicts a unit cell of the DC/SC superlattice; (ii) at $T_{SC}^{1D} \lesssim T_{SC}^{0D}$ the dots have grown and overlap to percolate the system in a connected network as in Fig. 2(d); (iii) ultimately, at $T_{SC}^{2D} \lesssim T_{SC}^{1D}$ the whole system becomes superconducting. (The SC boundaries in the phase diagram correspond to T_{SC}^{0D}.) The coupling proposed in Eq. (3) therefore predicts that, depending on the temperature, the SC order can have either a 0D, 1D, or 2D character. This can be directly probed with temperature-dependent local spectroscopy across the SC transition. In the absence of other pairing mechanisms, this picture predicts that if the penetration length of $\Phi(\mathbf{r})$ into the C region is smaller than L, it is possible to have $T_{SC}^{2D} = 0$ in the NC region of the phase diagram. SC would then span the system, at most, through the 1D network defined by the DCs.

The area of SC stability in the phase diagram depends on whether the parameter a_1 in Eq. (3) varies with E. If it does not, SC persists from the NC to the IC limit at temperatures below the gray line in Fig. 1. It remains in the IC limit because $|\nabla\psi_j|$ is finite, thereby supporting uniform SC. In the specific case of doped $TiSe_2$, however, SC exists only in a dome-shaped portion of the phase diagram, over a finite density range [1,5]. This phenomenology can be captured by replacing $a_1 \to a_1 E$ in the parameter a_s, making it depend both implicitly (through ψ_j) and explicitly on the lock-in parameter E. This amounts to making the coupling to CDW fluctuations weaker at higher densities, which is physically plausible in view of screening. The SC boundary numerically recalculated in this way drops to lower temperature when $E \to 0$, as conveyed by the red line in Fig. 1, which qualitatively reproduces the experimental SC dome (see also Fig. S3).

Ramifications. The feasibility of nonuniform percolative SC in the NC regime is determined by the characteristic width of DCs (w), their separation L (the size of C domains), and the SC coherence length ξ ($\sim$12 nm in $TiSe_2$ [36]). Likely, $w \lesssim \xi$, not sufficient to permit fully developed SC grains in the range $T_{SC}^{1D} < T < T_{SC}^{0D}$ where the model predicts nucleation at the vertices of the DC network.

The situation in the range $T_{SC}^{2D} < T < T_{SC}^{1D}$ has interesting implications in the presence of a magnetic field B. First, vortices are naturally pinned by the DC lattice, even in the absence of disorder, and their motion correlated. Second, given the likelihood that $w \lesssim \xi$, vortices would not squeeze within DCs; the supercurrent would instead circulate along a linked network of 1D SC channels [34], as illustrated in Fig. 3(b). If $L \gg \xi$, we may regard this as a microscopic version of SC wire grids [37–45], a distinctive feature of which are oscillatory dips as a function of B in thermodynamic [37] and transport [39] properties, with period determined by rational fractions ($f = \phi/\phi_0$) of the flux through the grid's elementary plaquette ($\phi \sim BL^2$, $\phi_0 \equiv h/2e$) [43,44,46].

It is tempting to speculate whether such a nonuniform SC texture can underlie the Little-Parks oscillations found in the SC phase of $TiSe_2$ near optimum doping [1]. To test it, assume the grid is hexagonal as in Fig. 2(d) ($f = 1/4$ [44]) and take the first experimental magnetoresistance dip at $B \simeq 0.13$ T. With our results, we obtain the incommensurability factor $\delta \sim 0.01$ and a typical distance between DCs $L \sim 70$ nm [47]. Compellingly, x-ray diffraction does reveal $\delta \sim 5\%$–15% in the superconducting dome [7], and STM finds DCs separated by tens of nm at optimum doping above T_{sc} [2]. It is noteworthy how these estimates agree with experiments.

Our model captures qualitatively well the emergence of SC correlated with the suppression of the C-CDW. This phenomenology is not unique to $TiSe_2$, but documented across a number of $2H$ and $1T$ TMDs [4] spanning both good metals and semimetals, as well as distinct commensurability conditions. Our approach straightforwardly extends to those cases [20], providing a definite and universal phenomenological foundation to further explore the interplay between these two coexisting orders and their fluctuations.

V.M.P. was supported by the Ministry of Education of Singapore through Grant No. MOE2015-T2-2-059 and AHCN by the National Research Foundation of Singapore under its Medium-Sized Centre Programme. Numerical computations were carried out at the HPC facilities of the NUS Centre for Advanced 2D Materials.

[1] L. J. Li, E. C. T. O'Farrell, K. P. Loh, G. Eda, B. Özyilmaz, and A. H. Castro Neto, Nature (London) **529**, 185 (2015).

[2] S. Yan, D. Iaia, E. Morosan, E. Fradkin, P. Abbamonte, and V. Madhavan, Phys. Rev. Lett. **118**, 106405 (2017).

[3] A. M. Novello, M. Spera, A. Scarfato, A. Ubaldini, E. Giannini, D. R. Bowler, and C. Renner, Phys. Rev. Lett. **118**, 017002 (2017).

[4] B. Wang, Y. Liu, K. Ishigaki, K. Matsubayashi, J. Cheng, W. Lu, Y. Sun, and Y. Uwatoko, Phys. Rev. B **95**, 220501 (2017).

[5] E. Morosan, H. W. Zandbergen, B. S. Dennis, J. W. G. Bos, Y. Onose, T. Klimczuk, A. P. Ramirez, N. P. Ong, and R. J. Cava, Nat. Phys. **2**, 544 (2006).

[6] Y. I. Joe, X. M. Chen, P. Ghaemi, K. D. Finkelstein, G. A. de la Peña, Y. Gan, J. C. T. Lee, S. Yuan, J. Geck, G. J. MacDougall, T. C. Chiang, S. L. Cooper, E. Fradkin, and P. Abbamonte, Nat. Phys. **10**, 421 (2014).

[7] A. Kogar, G. A. de la Pena, S. Lee, Y. Fang, S. X.-L. Sun, D. B. Lioi, G. Karapetrov, K. D. Finkelstein, J. P. C. Ruff, P. Abbamonte, and S. Rosenkranz, Phys. Rev. Lett. **118**, 027002 (2017).

[8] A. F. Kusmartseva, B. Sipos, H. Berger, L. Forró, and E. Tutiš, Phys. Rev. Lett. **103**, 236401 (2009).

[9] L. Li, C. Chen, K. Watanabe, T. Taniguchi, Y. Zheng, Z. Xu, V. M. Pereira, K. P. Loh, and A. H. C. Neto, arXiv:1803.10936.

[10] M. Spera, A. Scarfato, E. Giannini, and C. Renner, arXiv:1710.04096.

[11] H. Barath, M. Kim, J. F. Karpus, S. L. Cooper, P. Abbamonte, E. Fradkin, E. Morosan, and R. J. Cava, Phys. Rev. Lett. **100**, 106402 (2008).

[12] C. Chen, B. Singh, H. Lin, and V. M. Pereira, Phys. Rev. Lett. **121**, 226602 (2018).

[13] W. L. McMillan, Phys. Rev. B **14**, 1496 (1976).

[14] P. Bak and V. J. Emery, Phys. Rev. Lett. **36**, 978 (1976).

[15] G. Grüner, *Density Waves in Solids* (Addison-Wesley, Boston, 1994).

[16] R. E. Thomson, B. Burk, A. Zettl, and J. Clarke, Phys. Rev. B **49**, 16899 (1994).

[17] W. A. Little and R. D. Parks, Phys. Rev. Lett. **9**, 9 (1962).

[18] W. L. McMillan, Phys. Rev. B **16**, 4655 (1977).

[19] K. Nakanishi and H. Shiba, J. Phys. Soc. Jpn. **45**, 1147 (1978).

[20] See Supplemental Material at http://link.aps.org/supplemental/10.1103/PhysRevB.99.121108 for expanded details and additional discussion, which includes Refs. [1–3,6,7,12–14,18–21,23,25,26,29–34,48–54].

[21] W. L. McMillan, Phys. Rev. B **12**, 1187 (1975).

[22] F. J. Di Salvo, D. E. Moncton, and J. V. Waszczak, Phys. Rev. B **14**, 4321 (1976).

[23] P. Chen, Y.-H. Chan, X.-Y. Fang, Y. Zhang, M.-Y. Chou, S.-K. Mo, Z. Hussain, A.-V. Fedorov, and T.-C. Chiang, Nat. Commun. **6**, 8943 (2015).

[24] Disorder can introduce additional effects not seen in the experimental cases we consider; see Refs. [55,56].

[25] A. E. Jacobs and M. B. Walker, Phys. Rev. B **21**, 4132 (1980).

[26] K. Nakanishi and H. Shiba, J. Phys. Soc. Jpn. **43**, 1839 (1977).

[27] The actual magnitude of $\mathbf{q}_j^I$ does not play a role in the subsequent energy minimization because it can be absorbed into the definition of B.

[28] The form of interactions between density waves here is specific to the case of $TiSe_2$.

[29] K. Nakanishi, H. Takater, Y. Yamada, and H. Shiba, J. Phys. Soc. Jpn. **43**, 1509 (1977).

[30] K. Nakanishi and H. Shiba, J. Phys. Soc. Jpn. **44**, 1465 (1978).

[31] P. A. Lee, T. M. Rice, and P. W. Anderson, Solid State Commun. **14**, 703 (1974).

[32] A. Kotani, J. Phys. Soc. Jpn. **42**, 408 (1977).

[33] A. Kotani, J. Phys. Soc. Jpn. **42**, 416 (1977).

[34] M. Tinkham, *Introduction to Superconductivity*, 2nd ed. (McGraw-Hill, New York, 1996).

[35] The SC boundary in Fig. 1 was obtained with $a_0 = 10t + 60$ and $b_s = c_s = 1$.

[36] E. Morosan, L. Li, N. P. Ong, and R. J. Cava, Phys. Rev. B **75**, 104505 (2007).

[37] B. Pannetier, J. Chaussy, R. Rammal, and J. C. Villegier, Phys. Rev. Lett. **53**, 1845 (1984).

[38] H. D. Hallen, R. Seshadri, A. M. Chang, R. E. Miller, L. N. Pfeiffer, K. W. West, C. A. Murray, and H. F. Hess, Phys. Rev. Lett. **71**, 3007 (1993).

[39] X. S. Ling, H. J. Lezec, M. J. Higgins, J. S. Tsai, J. Fujita, H. Numata, Y. Nakamura, Y. Ochiai, C. Tang, P. M. Chaikin, and S. Bhattacharya, Phys. Rev. Lett. **76**, 2989 (1996).

[40] M. D. Stewart, A. Yin, J. M. Xu, and J. M. Valles, Science **318**, 1273 (2007).

[41] S. Teitel and C. Jayaprakash, Phys. Rev. Lett. **51**, 1999 (1983).

[42] S. Alexander, Phys. Rev. B **27**, 1541 (1983).

[43] Q. Niu and F. Nori, Phys. Rev. B **39**, 2134 (1989).

[44] Y.-L. Lin and F. Nori, Phys. Rev. B **65**, 214504 (2002).

[45] J. Berger and J. Rubinstein, *Connectivity and Superconductivity*, Vol. 62 (Springer, Berlin, 2001).

[46] K. Park and D. A. Huse, Phys. Rev. B **64**, 134522 (2001).

[47] Since $a = 0.35$ nm for $TiSe_2$ and $\eta \sim 1$ (Fig. 1), we have $L = \sqrt{3}a/(\eta\delta) = [\phi_0/(2\sqrt{3}B)]^{1/2} \simeq 70$ nm and $\delta \sim 0.01$.

[48] S. A. Jackson, P. A. Lee, and T. M. Rice, Phys. Rev. B **17**, 3611 (1978).

[49] M. Leroux, I. Errea, M. Le Tacon, S.-M. Souliou, G. Garbarino, L. Cario, A. Bosak, F. Mauri, M. Calandra, and P. Rodière, Phys. Rev. B **92**, 140303 (2015).

[50] D. B. McWhan, R. M. Fleming, D. E. Moncton, and F. J. DiSalvo, Phys. Rev. Lett. **45**, 269 (1980).

[51] D. E. Moncton, J. D. Axe, and F. J. DiSalvo, Phys. Rev. Lett. **34**, 734 (1975).

[52] C. Monney, E. F. Schwier, M. G. Garnier, N. Mariotti, C. Didiot, H. Cercellier, J. Marcus, H. Berger, A. N. Titov, H. Beck, and P. Aebi, New J. Phys. **12**, 125019 (2010).

[53] A. H. Castro Neto, Phys. Rev. Lett. **86**, 4382 (2001).

[54] B. Sipos, A. F. Kusmartseva, A. Akrap, H. Berger, L. Forró, and E. Tutiš, Nat. Mater. **7**, 960 (2008).

[55] J. S. Chen, J. K. Wang, S. V. Carr, S. C. Vogel, O. Gourdon, P. Dai, and E. Morosan, Phys. Rev. B **91**, 045125 (2015).

[56] A. Banerjee, A. Garg, and A. Ghosal, Phys. Rev. B **98**, 104206 (2018).